Dalton Transactions

PAPER

View Article Online
View Journal | View Issue

Cite this: *Dalton Trans.*, 2014, **43**, 17274

Neutral redox-active hydrogen- and halogen-bonding [2]rotaxanes for the electrochemical sensing of chloride†

Jason Y. C. Lim,[a] Matthew J. Cunningham,[b] Jason J. Davis[b] and Paul D. Beer*[a]

Received 26th August 2014,
Accepted 2nd October 2014

DOI: 10.1039/c4dt02591a

www.rsc.org/dalton

The first examples of redox-active ferrocene-functionalised *neutral* [2]rotaxanes have been synthesised *via* chloride anion templation. ^{1}H NMR spectroscopic titrations reveal that these [2]rotaxane host systems recognize chloride selectively over other halides and oxoanions in highly-competitive aqueous media. By replacing the hydrogen bonding prototriazole units of the rotaxane axle component with iodotriazole halogen bond-donor groups, the degree of chloride selectivity of the [2]rotaxanes is modulated. Electrochemical voltammetric experiments demonstrate that the rotaxanes can sense chloride *via* cathodic perturbations of the respective rotaxanes' ferrocene–ferrocenium redox-couple upon anion addition.

Introduction

Anions are ubiquitous and their importance in biology and the environment resulting from anthropogenic activities is well established. This continues to stimulate the growth of anion detection and binding in supramolecular chemistry.[1–3] While artificial anion receptors have yet to achieve the remarkable selectivities found in nature, interlocked host molecules such as rotaxanes, more commonly employed for potential molecular machine-like nanotechnological applications,[4,5] have emerged as promising candidates for anion binding and sensing in recent years.[6] Their unique positively-charged three dimensional topological cavities, containing convergent hydrogen bonding and halogen bond donor groups, facilitate the selective encapsulation of the anionic guest species in highly-competitive aqueous solvent media.[7,8] We have recently demonstrated that *neutral* [2]rotaxane host analogues are also capable of recognizing halide anions, with binding affinities comparable to charged pyridinium axle component rotaxane systems.[9] The integration of redox-active reporter groups into interlocked structural frameworks also empowers such systems to sense anions by means of electrochemical methodologies.[6]

Herein, we describe the synthesis of a series of unprecedented *neutral* redox-active [2]rotaxanes containing a ferrocene-appended macrocycle unit, and demonstrate their ability to selectively recognise and electrochemically sense chloride in preference to bromide and oxoanions. Motivated by our earlier discoveries that halogen bond-donors can profoundly influence the selectivity of anion recognition,[10] the effect of incorporating the halogen bond donor iodotriazole motif into the axle component of a redox-active rotaxane on anion recognition and subsequent electrochemical sensing is also investigated.

Experimental

General

All commercially available chemicals and solvents were used as received without further purification. All dry solvents were thoroughly degassed with N_2, dried through a Mbraun MPSP-800 column and used immediately. Triethylamine was distilled and stored over potassium hydroxide pellets. Deionised water was used in all cases. All tetrabutylammonium salts used for anion titrations were stored in vacuum desiccators prior to use.

NMR spectra were recorded on Bruker AVIII HD Nanobay 400 MHz, Bruker AVIII 500 MHz and Bruker AVIII 500 MHz (with ^{13}C cryoprobe) spectrometers. Electrospray ionisation mass spectrometry (ESI-MS) was performed using the Waters Micromass LCT and Bruker microTOF spectrometers.

Synthesis

Compounds **3**,[11] **4**,[12] **8**,[13] **9a**[14] and **9b**[15] were synthesised according to literature procedures. Procedures for the preparation of the ferrocene-appended macrocycles **7a–d** are detailed in the ESI.†

5-Ferrocene isophthalamide bis-azide macrocycle precursor (5). To a vigorously stirred suspension of 5-ferrocenyl isophthalic acid (**3**) (630 mg, 1.80 mmol) in dry CH_2Cl_2 (5 mL)

[a]*Chemistry Research Laboratory, Department of Chemistry, University of Oxford, Mansfield Road, Oxford, OX1 3TA, UK. E-mail: paul.beer@chem.ox.ac.uk*
[b]*Physical & Theoretical Chemistry Laboratory, South Parks Road, Oxford, OX1 3TA, UK*
† Electronic supplementary information (ESI) available. See DOI: 10.1039/c4dt02591a

containing catalytic quantities of dimethylformamide was added oxalyl chloride dropwise (0.46 mL, 5.40 mmol) under N_2. The reaction was stirred for 2 hours to obtain a clear red solution, which was evaporated to dryness *in vacuo* to yield the acid chloride as a dark red solid, which was then re-dissolved in dry CH_2Cl_2. This solution was added dropwise to a colourless solution of **4** (0.800 g, 3.60 mmol) in dry CH_2Cl_2 (50 mL) containing anhydrous triethylamine (1.50 mL, 10.8 mmol) and catalytic quantities of *N*,*N*-dimethylaminopyridine (DMAP) at 0 °C. The reaction was allowed to warm up to room temperature and stirred overnight. After which, the reaction mixture was washed successively with 10% HCl (20 mL) and water (2 × 20 mL). The combined organics were dried with $MgSO_4$ and the solvent removed *in vacuo* to form a sticky red-orange liquid. Silica gel chromatography (eluent: 6 : 4 EtOAc–petroleum ether) gave **5** as an orange solid (602 mg, 45%). **^{1}H NMR** (400 MHz, $CDCl_3$) δ 8.09 (2H, d, ^4J = 1.6 Hz, Ar*H*), 7.91 (1H, d, ^4J = 1.6 Hz, Ar*H*), 6.88 (8H, m, hydroquinone-*H*), 6.70 (2H, br. t, ^3J = 5.2 Hz, CON*H*), 4.73 (2H, t, ^3J = 1.6 Hz, Fc*H*), 4.40 (2H, t, ^3J = 1.6 Hz, Fc*H*), 4.16 (4H, t, ^3J = 4.8 Hz, –OCH_2CH$_2$N$_3$), 4.11 (4H, t, ^3J = 5.2 Hz, CONHCH$_2$CH_2O), 4.05 (5H, s, Fc*H*), 3.90 (4H, quart., ^3J = 5.2 Hz, CONHCH_2), 3.57 (4H, t, ^3J = 4.8 Hz, –CH_2N$_3$); **^{13}C NMR** (100 MHz, $CDCl_3$) δ 167.0, 153.1, 152.8, 141.5, 134.9, 127.5, 122.2, 115.8, 115.6, 83.3, 69.9, 69.9, 67.7, 67.3, 66.9, 50.2, 39.8; **MS** (ESI +ve) *m*/*z* 781.2137 ([M + Na]$^+$, $C_{38}H_{38}FeNaN_8O_6$, calc. 781.2157).

5-Ferrocene isophthalamide bis-amine macrocycle precursor (6). Ferrocene-appended bis-azide macrocycle precursor **5** (610 mg, 0.804 mmol) was dissolved in a minimum amount of methanol (*ca.* 30 mL), and 10% by weight Pd/C (150 mg) was added portionwise to the orange solution. Hydrazine monohydrate (0.13 mL, 4.02 mmol) was then added to the vigorously stirred suspension and the reaction heated under reflux for 7 hours. After cooling to ambient temperature, the reaction was filtered through celite, and the resulting orange solution was dried *in vacuo* to obtain **6** as an orange solid in quantitative yield. **^{1}H NMR** (400 MHz, $CDCl_3$) δ 8.01 (2H, s, Ar*H*), 7.91 (1H, s, Ar*H*), 6.86 (8H, dd, ^3J = 9.6 Hz, hydroquinone-*H*), 6.77 (2H, t, ^3J = 5.6 Hz, CON*H*), 4.73 (2H, s, Fc*H*), 4.39 (2H, s, Fc*H*), 4.15 (4H, t, ^3J = 4.8 Hz, CONHCH$_2$CH_2O), 4.04 (5H, s, Fc*H*), 3.94 (4H, t, ^3J = 4.8 Hz, OCH_2CH$_2$NH$_2$), 3.89 (4H, quart., ^3J = 4.8 Hz, CONHCH_2), 3.06 (4H, t, ^3J = 4.8 Hz, CH_2NH$_2$); **^{13}C NMR** (100 MHz, $CDCl_3$) δ 167.0, 153.5, 152.7, 141.4, 134.9, 127.4, 122.2, 115.5, 115.5 (repeat), 83.0, 70.7, 69.7, 69.7 (repeat), 67.3, 66.7, 41.6, 39.8; **MS** (ESI +ve) *m*/*z* 707.2528 ([M + H]$^+$, $C_{38}H_{43}FeN_4O_6$, calc. 707.2527).

Bis-prototriazole axle (10a). Pyridine *N*-oxide bis-azide **8** (120 mg, 0.345 mmol), alkyne **9a** (375 mg, 0.690 mmol), tris-[(1-benzyl-1*H*-1,2,3-triazol-4-yl)methyl]amine (TBTA) (73.0 mg, 0.138 mmol), diisopropyl-ethylamine (0.18 mL, 1.04 mmol) and tetrakis(acetonitrile)copper(I) hexafluorophosphate (43.4 mg, 0.138 mmol) were dissolved in CH_2Cl_2 (20 mL) with slight heating. The resulting reaction mixture was then cooled to ambient temperature, and stirred overnight under N_2 to give a cloudy green suspension. The reaction was washed with 10% aqueous ammonia (3 × 10 mL), and the aqueous layer was back-extracted with CH_2Cl_2 (2 × 10 mL). The combined organics were dried with $MgSO_4$ and dried *in vacuo* to give a pale green solid. Purification by silica gel chromatography (eluent: 4% CH_3OH in CH_2Cl_2) gave the product as a white solid (350 mg, 71%). **^{1}H NMR** (400 MHz, $CDCl_3$) δ 8.94 (2H, s, pyridine *N*-oxide Ar*H*), 8.34 (2H, t, ^3J = 6.2 Hz, CON*H*), 8.12 (1H, s, pyridine *N*-oxide Ar*H*), 7.53 (2H, s, triazole*H*), 7.12 (12H, d, ^3J = 8.3 Hz, stopper-Ar*H*), 6.97–7.02 (16H, m, stopper Ar*H*), 6.67 (4H, d, ^3J = 8.8 Hz, stopper Ar*H*), 4.96 (4H, s, –CH_2O), 4.38 (4H, t, ^3J = 6.2 Hz, –CH_2-triazole), 3.50 (4H, q, ^3J = 6.5 Hz, –CH_2NHCO), 2.22 (4H, t, ^3J = 6.0 Hz, –CH$_2$CH_2CH$_2$), 1.21 (54H, s, ^{t}Bu axle); **^{13}C NMR** (100 MHz, $CDCl_3$) δ 162.5, 156.0, 146.4, 144.0, 140.5, 133.6, 132.4, 130.7, 124.1, 123.5, 113.1, 63.1, 61.5, 48.5, 37.8, 34.3, 31.4, 29.3; **MS** (ESI +ve) *m*/*z* 1455.8480 ([M + Na]$^+$, $C_{93}H_{109}N_9NaO_5$, calc. 1455.8510).

Bis-iodotriazole axle (10b). Pyridine *N*-oxide bis-azide **8** (21 mg, 0.061 mmol) and iodoalkyne stopper **9b** (81 mg, 0.121 mmol) were dissolved in THF (3 mL) with heating, and allowed to cool to ambient temperature before copper(I) iodide (1.2 mg, 0.0061 mmol) and TBTA (3.2 mg, 0.0061 mmol) were added portionwise. The reaction was stirred overnight under N_2, following which the reaction mixture was washed with 10% aqueous ammonia (2 × 5 mL) and the aqueous layer back-extracted with chloroform (2 × 10 mL). The combined organic layer was dried with $MgSO_4$ and solvent removed to give a pale green solid. Silica gel chromatographic purification (eluent: 5% CH_3OH in CH_2Cl_2) gave the product as a white solid (61 mg, 60%). **^{1}H NMR** (400 MHz, $CDCl_3$) δ 9.10 (2H, s, pyridine *N*-oxide Ar*H*), 8.39 (2H, t, ^3J = 5.6 Hz, CON*H*), 8.35 (1H, s, pyridine *N*-oxide Ar*H*), 7.22 (12H, d, ^3J = 8.4 Hz, stopper Ar*H*), 7.10–7.06 (16H, m, stopper Ar*H*), 6.82 (4H, d, ^3J = 9.2 Hz, stopper Ar*H*), 4.99 (4H, s, –OCH_2), 4.49 (4H, t, ^3J = 6.6 Hz, –CH_2-iodotriazole), 3.55 (4H, quart., ^3J = 5.6 Hz, –CH_2NHCO), 2.30 (4H, quint., ^3J = 6.0 Hz, –CH$_2$CH_2CH$_2$), 1.29 (54H, s, ^{t}Bu); **^{13}C NMR** (100 MHz, $CDCl_3$) δ 162.5, 156.1, 148.3, 147.7, 144.0, 140.5, 140.3, 133.7, 132.4, 130.7, 124.1, 113.3, 81.3, 63.1, 61.5, 48.8, 37.6, 34.3, 31.4, 28.7; **MS** (ESI +ve) *m*/*z* 1706.6375 ([M + Na]$^+$, $C_{93}H_{107}I_2N_9NaO_5$, calc. 1706.6377).

General protocol for synthesis of [2]rotaxanes (1a–e)

In all cases, the appropriate axle (**10a** or **10b**), bis-amine macrocycle precursor **6** and the appropriate isophthalic acid were used in a 1 : 1 : 1 mole ratio. Firstly, the isophthalic acid (1.0 eq.) was suspended in dry CH_2Cl_2 (2 mL) containing a drop of DMF. Oxalyl chloride (3.0 eq.) was added dropwise and the reaction was stirred for 4 hours till a clear solution was obtained. The solvent was removed and the yellow bis-acid chloride was thoroughly dried under vacuum before being redissolved in dry CH_2Cl_2 (5 mL) and taken up in a syringe. The appropriate axle, **6**, and dry triethylamine (4.0 eq.) were dissolved in dry CH_2Cl_2 (30 mL), and the bis-acid chloride solution was added dropwise over 30 minutes. The resulting clear orange reaction mixture was stirred under N_2 overnight. Following which, the organic layer was washed successively with 1 M citric acid (20 mL), saturated aqueous $NaHCO_3$ (20 mL) and water (10 × 20 mL), before being dried with

$MgSO_4$. The solvent was removed *in vacuo* to give an orange solid, which was purified using preparatory thin layer chromatography to give the desired [2]rotaxane as an orange solid.

***tert*-Butyl-functionalised, bis-prototriazole rotaxane (1a).** Using *tert*-butyl isophthalic acid (18.8 mg, 0.085 mmol), oxalyl chloride (0.022 mL, 0.26 mmol), axle **10a** (124 mg, 0.085 mmol), bisamine **6** (60 mg, 0.085 mmol) and triethylamine (0.047 mL, 0.34 mmol) yielded **1a** (32 mg, 16%). **^{1}H NMR** (500 MHz, $CDCl_3$–d^4-MeOD 1 : 1) δ 8.44 (2H, s, pyridine *N*-oxide Ar*H*), 8.42 (1H, s, Fc-Ar*H*), 8.39 (1H, s, ^{t}Bu-Ar*H*), 8.11 (2H, s, Fc-Ar*H*), 8.10 (1H, s, pyridine *N*-oxide Ar*H*), 8.10 (2H, s, ^{t}Bu-Ar*H*), 7.82 (2H, s, triazole*H*), 7.20 (12H, d, ^3J = 8.3 Hz, stopper-Ar*H*), 7.05 (16H, m, stopper Ar*H*), 6.80 (4H, d, ^3J = 8.8 Hz, stopper Ar*H*), 6.37 (8H, s, hydroquinone Ar*H*), 5.06 (4H, s, –OCH_2 axle), 4.84 (2H, br. s, Fc*H*), 4.41 (2H, br. s, Fc*H*), 4.21 (4H, t, ^3J = 6.5 Hz, –CH_2-triazole axle), 4.10 (5H, s, Fc*H*), 3.97 (8H, m, –CH_2O macrocycle), 3.73 (8H, m, –CONHCH_2 macrocycle), 3.26 (4H, t, ^3J = 6.5 Hz, –CH_2NHCO axle), 2.04 (4H, t, ^3J = 6.5 Hz, –$CH_2CH_2CH_2$ axle), 1.34 (9H, s, ^{t}Bu macrocycle), 1.27 (54H, s, ^{t}Bu axle); **^{13}C NMR** (125 MHz, $CDCl_3$–d^4-MeOD 1 : 1) δ 169.1, 168.7, 162.7, 156.6, 153.2, 148.9, 144.7, 142.0, 140.9, 140.0, 134.7, 134.4, 133.1, 132.9, 131.2, 128.9, 128.7, 124.6, 123.1, 115.5, 113.7, 67.1, 63.6, 62.0, 40.8, 37.7, 35.6, 34.8, 31.7, 31.5, 30.4, 30.2; **MS** (ESI +ve) *m*/*z* 2348.1594 ([M + Na]$^+$, $C_{143}H_{161}FeN_{13}NaO_{13}$, calc. 2348.1613).

Bis-ferrocene functionalised bis-prototriazole rotaxane (1b). 5-Ferrocene isophthalic acid (20 mg, 0.057 mmol), oxalyl chloride (0.015 mL, 0.171 mmol), axle **10a** (81 mg, 0.057 mmol), bisamine **6** (40 mg, 0.057 mmol) and triethylamine (0.032 mL, 0.23 mmol) gave **1b** (30 mg, 22%). **^{1}H NMR** (500 MHz, $CDCl_3$–d^4-MeOD 1 : 1) δ 8.41 (2H, s, pyridine *N*-oxide Ar*H*), 8.37 (2H, s, Fc-isophthalamide Ar*H*), 8.14 (4H, s, Fc-isophthalamide Ar*H*), 8.06 (1H, s, pyridine *N*-oxide Ar*H*), 7.72 (2H, s, triazole*H*), 7.19 (12H, d, ^3J = 8.5 Hz, stopper-Ar*H*), 7.05 (16H, m, stopper Ar*H*), 6.79 (4H, d, ^3J = 8.8 Hz, stopper Ar*H*), 6.37 (8H, s, hydroquinone Ar*H*), 5.03 (4H, s, –OCH_2 axle), 4.75 (4H, s, Fc*H*), 4.33 (4H, s, Fc*H*), 4.20 (4H, t, ^3J = 6.5 Hz, –CH_2-triazole axle), 4.01 (10H, s, Fc*H*), 3.97 (8H, m, –CH_2O macrocycle), 3.74 (8H, m, –CONHCH_2 macrocycle), 3.25 (4H, t, ^3J = 6.5 Hz, –CH_2NHCO), 2.04 (4H, t, ^3J = 6.5 Hz, –$CH_2CH_2CH_2$ axle), 1.26 (54H, s, ^{t}Bu axle); **^{13}C NMR** (125 MHz, $CDCl_3$–d^4-MeOD 1 : 1) δ 168.7, 162.7, 156.6, 153.2, 148.9, 144.7, 142.0, 141.0, 140.0, 134.9, 133.1, 132.9, 131.3, 128.8, 124.6, 124.2, 123.0, 115.6, 113.7, 83.6, 70.3, 67.3, 63.6, 62.0, 48.5, 40.8, 37.8, 34.8, 31.8, 30.4; **MS** (ESI +ve) *m*/*z* 2475.0965 ([M + Na]$^+$, $C_{149}H_{161}Fe_2N_{13}NaO_{13}$, calc. 2475.0928).

Pyridine-functionalised, bis-prototriazole rotaxane (1c). 3,5-Pyridine dicarboxylic acid (12 mg, 0.070 mmol), oxalyl chloride (0.018 mL, 0.21 mmol), axle **10a** (100 mg, 0.070 mmol), bisamine **6** (49 mg, 0.070 mmol) and triethylamine (0.040 mL, 0.28 mmol) gave **1c** (14 mg, 9%). **^{1}H-NMR** (500 MHz, $CDCl_3$–d^4-MeOD 1 : 1) δ 9.15 (2H, s, macrocycle pyridine Ar*H*), 8.96 (1H, s, macrocycle pyridine Ar*H*), 8.45 (2H, s, axle pyridine *N*-oxide Ar*H*), 8.36 (1H, s, Fc-Ar*H*), 8.13 (2H, s, Fc-Ar*H*), 8.07 (1H, s, pyridine *N*-oxide Ar*H*), 7.80 (2H, s, triazole-*H*), 7.19 (12H, d, ^3J = 8.5 Hz, stopper-Ar*H*), 7.05 (16H, m, stopper Ar*H*), 6.79 (4H, d, ^3J = 8.8 Hz, stopper Ar*H*), 6.39 (8H, m, hydroquinone Ar*H*), 5.05 (4H, s, –OCH_2 axle), 4.75 (2H, s, Fc*H*), 4.33 (2H, s, Fc*H*), 4.25 (4H, t, ^3J = 6.7 Hz, –CH_2-triazole axle), 4.00 (5H, s, Fc*H*), 3.95–3.98 (8H, m, –CH_2O macrocycle), 3.72–3.74 (8H, m, –CONHCH_2 macrocycle), 3.26 (4H, t, ^3J = 6.7 Hz, –CH_2NHCO), 2.06 (4H, t, ^3J = 6.8 Hz, –$CH_2CH_2CH_2$ axle), 1.27 (54H, s, ^{t}Bu axle); **^{13}C-NMR** (125 MHz, $CDCl_3$–d^4-MeOD 1 : 1) δ 169.1, 166.9, 163.1, 157.0, 153.7, 153.5, 152.1, 149.2, 145.0, 145.0 (repeat), 124.4, 141.3, 140.4, 135.3, 134.7, 133.6, 133.2, 131.6, 130.5, 128.9, 126.6, 124.9, 124.7, 123.6, 116.0, 114.1, 83.9, 70.6, 70.6 (repeat), 67.6, 67.5, 64.0, 62.3, 50.0, 40.9, 38.1, 35.0, 32.1, 32.0, 30.6, 29.6; **MS** (ESI +ve) *m*/*z* 2292.0956 ([M + Na]$^+$, $C_{138}H_{152}FeN_{14}NaO_{13}$, calc. 2292.0905).

Nitro-functionalised, bis-prototriazole rotaxane (1d). 5-Nitro isophthalic acid (15 mg, 0.070 mmol), oxalyl chloride (0.018 mL, 0.21 mmol), axle **10a** (100 mg, 0.070 mmol), bisamine **6** (49 mg, 0.070 mmol) and triethylamine (0.040 mL, 0.28 mmol) gave **1d** (32 mg, 20%). **^{1}H-NMR** (500 MHz, $CDCl_3$–d^4-MeOD 1 : 1) δ 8.97 (1H, s, NO_2-Ar*H*), 8.88 (2H, s, NO_2-Ar*H*), 8.45 (2H, s, pyridine *N*-oxide Ar*H*), 8.37 (1H, s, Fc-Ar*H*), 8.14 (2H, s, Fc-Ar*H*), 8.08 (1H, s, pyridine *N*-oxide Ar*H*), 7.78 (2H, s, triazole*H*), 7.19 (12H, d, ^3J = 8.5 Hz, stopper-Ar*H*), 7.05 (16H, m, stopper Ar*H*), 6.79 (4H, d, ^3J = 8.8 Hz, stopper Ar*H*), 6.41–6.37 (8H, m, hydroquinone Ar*H*), 5.04 (4H, s, –OCH_2 axle), 4.74 (2H, s, Fc*H*), 4.33 (2H, s, Fc*H*), 4.25 (4H, t, ^3J = 6.5 Hz, –CH_2-triazole axle), 4.00 (5H, s, Fc*H*), 3.99 (8H, m, –CH_2O macrocycle), 3.74 (8H, m, –CONHCH_2 macrocycle), 3.26 (4H, t, ^3J = 6.5 Hz, –CH_2NHCO), 2.06 (4H, t, ^3J = 6.5 Hz, –$CH_2CH_2CH_2$ axle), 1.26 (54H, s, ^{t}Bu axle); **^{13}C-NMR** (125 MHz, $CDCl_3$–d^4-MeOD 1 : 1) δ 168.9, 166.5, 162.9, 156.7, 153.5, 153.3, 149.4, 149.0, 144.8, 144.8 (repeated), 142.4, 141.1, 140.2, 136.8, 135.1, 133.4, 133.0, 131.9, 131.4, 128.7, 126.4, 126.2, 124.7, 124.5, 123.3, 116.2, 115.8, 115.7, 113.8, 83.7, 70.4, 70.3, 67.3, 63.7, 62.0, 40.9, 40.8, 37.9, 34.8, 31.8, 30.4, 29.4; **MS** (ESI +ve) *m*/*z* 2336.0797 ([M + Na]$^+$, $C_{139}H_{152}FeN_{14}NaO_{15}$, calc. 2336.0803).

***tert*-Butyl-functionalised, bis-iodotriazole rotaxane (1e).** *tert*-Butyl isophthalic acid (19 mg, 0.085 mmol), oxalyl chloride (0.022 mL, 0.26 mmol), axle **10b** (143 mg, 0.085 mmol), bisamine **6** (60 mg, 0.085 mmol) and triethylamine (0.047 mL, 0.34 mmol) gave **13** (13 mg, 6%). **^{1}H-NMR** (500 MHz, $CDCl_3$–d^4-MeOD 1 : 1) δ 8.48 (2H, s, pyridine *N*-oxide Ar*H*), 8.38 (1H, s, Fc-Ar*H*), 8.37 (1H, s, ^{t}Bu-Ar*H*), 8.15 (2H, s, Fc-Ar*H*), 8.14 (1H, s, pyridine *N*-oxide Ar*H*), 8.13 (2H, s, ^{t}Bu-Ar*H*), 7.20 (12H, d, ^3J = 8.6 Hz, stopper-Ar*H*), 7.07–7.04 (16H, m, stopper Ar*H*), 6.81 (4H, d, ^3J = 8.9 Hz, stopper Ar*H*), 6.40 (8H, m, hydroquinone Ar*H*), 4.92 (4H, s, –OCH_2 axle), 4.76 (2H, s, Fc*H*), 4.37 (2H, s, Fc*H*), 4.21 (4H, t, ^3J = 7.0 Hz, –CH_2-triazole axle), 4.00 (5H, s, Fc*H*), 3.97 (8H, m, –CH_2O macrocycle), 3.73 (8H, m, –CONHCH_2 macrocycle), 3.29 (4H, t, ^3J = 6.9 Hz, –CH_2NHCO axle), 2.04 (4H, t, ^3J = 6.9 Hz, –$CH_2CH_2CH_2$ axle), 1.35 (9H, s, ^{t}Bu macrocycle), 1.27 (54H, s, ^{t}Bu axle); **^{13}C-NMR** (125 MHz, $CDCl_3$–d^4-MeOD 1 : 1) δ 169.3, 168.9, 163.0, 156.9, 153.4, 153.3, 149.1, 148.2, 144.9, 142.2, 141.2, 140.3, 135.1, 134.7, 133.5, 133.0, 131.4, 129.0, 128.8, 126.8, 124.8, 123.6, 123.5, 115.8, 114.1, 83.7, 83.0, 70.5, 70.4, 67.5, 67.5 (repeat), 67.4, 63.8, 62.1,

40.8, 38.0, 35.7, 34.9, 31.8, 31.6, 29.9; **MS** (ESI +ve) *m*/*z* 2598.9513 ($[M + Na]^+$, $C_{143}H_{159}FeI_2N_{13}NaO_{13}$, calc. 2598.9511).

Results and discussion

Synthesis of redox-active [2]rotaxanes

The target redox-active [2]rotaxane host design, shown in Fig. 1, consists of a pyridine *N*-oxide axle component interlocked with a bis-isophthalamide functionalised macrocycle, which is functionalized at one of the isophthalamide motifs with a ferrocene group.

Ferrocene appendage to an isophthalate ester motif was achieved *via* Sandmeyer-type coupling involving ferrocenium and 5-diazonium isophthalate ester,[11] as detailed in Scheme 1. Subsequent ester hydrolysis gave the corresponding 5-ferrocene isophthalic acid **3**, which, upon reaction with oxalyl chloride, afforded the bis-acid chloride. Condensation with two equivalents of amine **4** [12] produced the bis-azide macrocycle precursor **5** in 49% yield. Reduction of **5** using hydrazine monohydrate with 10% palladium loading on carbon allowed quantitative conversion to the bis-amine macrocycle precursor **6**. The synthesis of the ferrocene-appended macrocycles **7a–d** was achieved under high dilution conditions *via* amide condensation reactions between bis-amine **6** and bis-acid chlorides in yields ranging from 20–37%. However, with the exception of the *tert*-butyl functionalised macrocycle **7a**, all the cyclic products unexpectedly displayed poor solubility in low-polarity halogenated solvents. As a consequence, the previously reported anion-templated copper catalysed azide–alkyne cycloaddition (CuAAC) 'click' stoppering rotaxane synthesis of a pseudorotaxane assembly containing the pyridine *N*-oxide axle precursor component[9] could not be undertaken in chloroform solution.

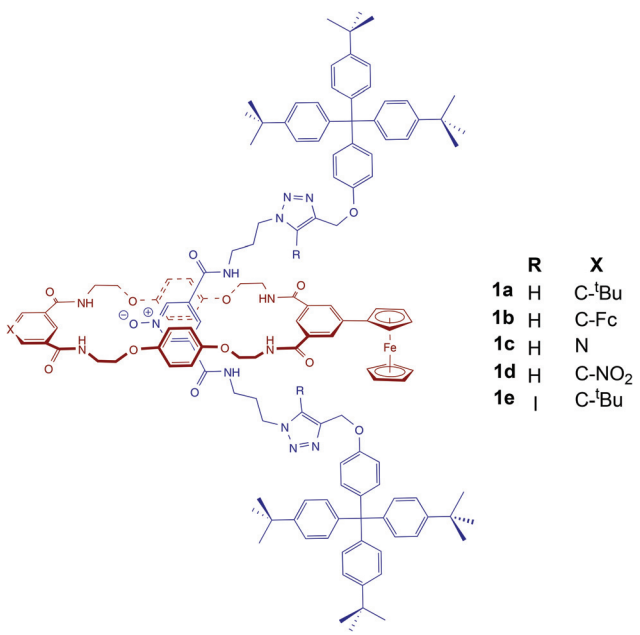

Fig. 1 Structure of target *neutral* ferrocene (Fc)-appended [2]rotaxanes **1a–e**.

Hence, a new chloride anion-templated clipping strategy for neutral rotaxane formation was used. As illustrated in Scheme 2, the proto- and iodotriazole-linked pyridine *N*-oxide axles **10a** and **10b** were prepared by the CuAAC reaction of pyridine *N*-oxide bis-azide **8** [13] and the alkyne functionalized terphenyl stoppers **9a** [14] and **9b** [15] respectively. The [2]rotaxanes were then prepared by condensation of bis-amine **6** with the appropriate bis-acid chloride derivative in the presence of an equimolar quantity of stoppered axle **10a** or **10b**. Removal of the templating chloride anion (generated *in situ* from the amide condensation reactions) from the rotaxane binding cavity was achieved by repeated washings with water to afford the charge-neutral [2]rotaxanes **1a–e** isolated in yields of up to 22% following purification by preparative thin layer chromatography. All five rotaxanes were characterised by ^{1}H and ^{13}C NMR spectroscopy and high resolution electrospray ionisation mass spectrometry (ESI-MS).

Evidence for the interlocked nature of the rotaxanes is provided by a comparison of their ^{1}H-NMR spectra with those of the free macrocycle and axle components (Fig. 2). Significant upfield shifts are seen for signals arising from the protons of the hydroquinones (*e* and *f*) of the macrocycle and the pyridine *N*-oxide of the axle (*i.e.* *m* and *n*). These arise from diagnostic aromatic donor–acceptor interactions between the macrocycle and the axle. Furthermore, distinct downfield shifts in the macrocycle internal isophthalamide protons *a* and *b* are observed, which arise due to hydrogen bonding interactions with the oxygen atom of the pyridine *N*-oxide axle. Although only one of these protons can interact with the pyridine *N*-oxide oxygen atom at any one time, there are approximately equal perturbations of protons *a* and *b* for all the [2]rotaxanes bearing asymmetric macrocycles (**1a** and **1c–e**), which is indicative of the macrocycle pirouetting around the axle in a dynamic fashion which is fast on the NMR timescale.‡ Finally, numerous through-space interactions were observed between the macrocycle and axle components of all rotaxanes in their two-dimensional ^{1}H–^{1}H ROESY spectra (see ESI†), giving conclusive evidence of their interlocked nature.

Anion recognition studies

^{1}H NMR titrations. The anion binding properties of the neutral [2]rotaxanes were investigated using ^{1}H-NMR titration experiments in the highly competitive solvent mixture 45 : 45 : 10 $CDCl_3$–CD_3OD–D_2O.

The addition of tetrabutylammonium (TBA) chloride to the prototriazole-bearing [2]rotaxanes **1a–d** caused the proton signals for macrocycle isophthalamide protons *a* and *b*, as

‡Further evidence of this pirouetting motion is provided by the fact that unlike many pyridinium axle rotaxanes,[13,16] no splitting of the hydroquinone ^{1}H-NMR signals was observed following rotaxane formation, which is indicative of co-conformational dynamic behaviour being fast on the NMR timescale.

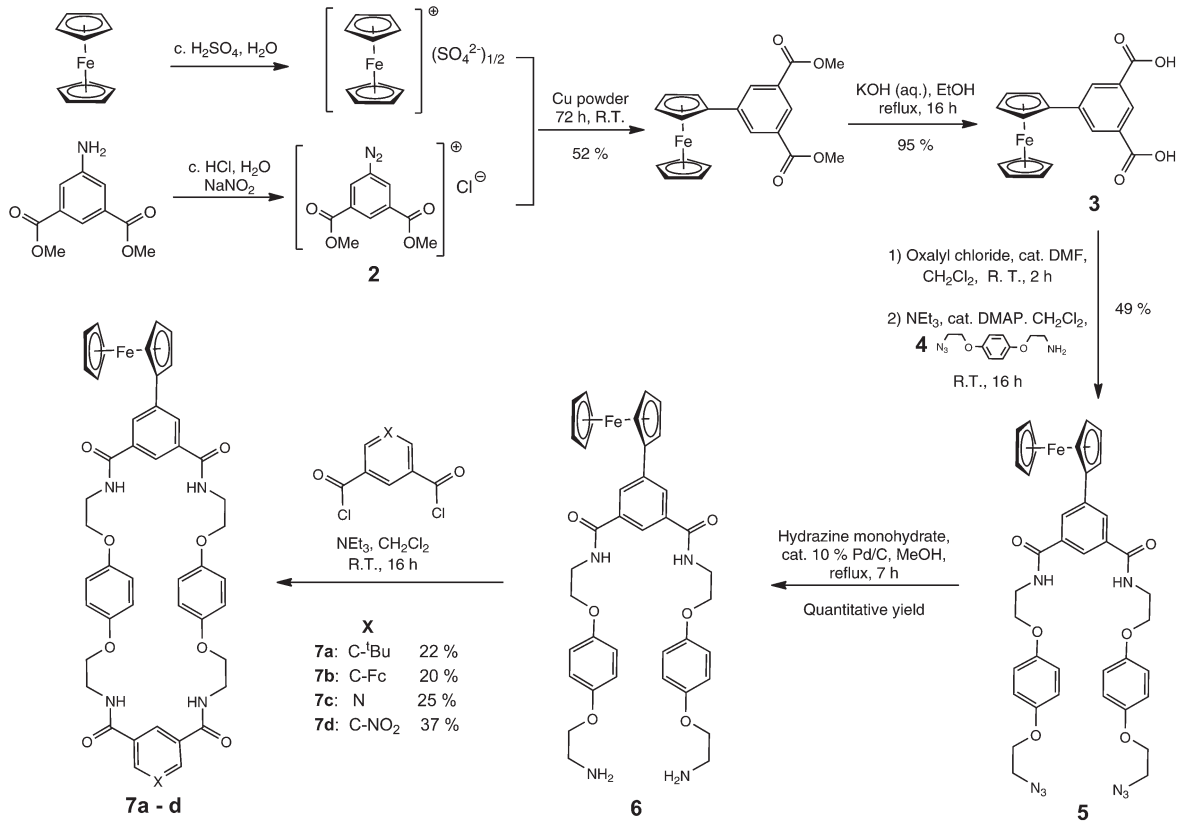

Scheme 1 Synthesis of ferrocene-appended macrocycles.

well as the pyridine *N*-oxide proton *m* to undergo significant downfield shifts (Fig. 3). These arise from hydrogen bonding interactions with the chloride anion residing within the interlocked binding cavity of the rotaxanes. Interestingly, no difference in the magnitude of perturbation was observed between macrocycle protons *a* and *b*, suggesting that there is no preference for chloride binding at either isophthalamide unit. Similar downfield shifts were observed for the respective rotaxanes' axle prototriazole protons as well, confirming their involvement in anion binding as a result of the axle wrapping around the interlocked cavity bound chloride anion. Upfield perturbations of the hydroquinone proton signals *e* and *f* are seen, indicating that chloride binding increases the strength of aromatic donor–acceptor interactions between the macrocycle's electron rich hydroquinone groups and the electron deficient pyridine *N*-oxide axle motif. Analogous titration experiments with bromide and iodide resulted in similar perturbations of the respective rotaxanes' proton signals, although they were of smaller magnitude. By contrast, no significant shifts were observed on addition of dihydrogen phosphate (Fig. 4) and acetate which suggests these oxoanions are not bound by the rotaxanes; presumably they are too large to be encapsulated by the interlocked host cavity. WinEQNMR2[17] analysis of the halide titration data monitoring the chemical shift of the internal isophthalamide proton of the pyridine *N*-oxide axle component (Fig. 4) determined 1 : 1 stoichiometric association constant values shown in Table 1.§

All the rotaxanes exhibit the selectivity trend of chloride > bromide > iodide, in spite of chloride being the most heavily solvated halide in this aqueous solvent mixture following the Hofmeister series.[18] This suggests that the rotaxanes' interlocked cavity is of complementary size for chloride anion recognition. Interestingly, the halide anion association constants of the prototriazole-[2]rotaxanes **1a–d** generally show little variation regardless of the substituent on the macrocycle isophthalamide motif. This indicates that the dynamic nature of these rotaxanes enable the halide to bind at either macrocycle component isophthalamide anion recognition site.

We have previously demonstrated that introducing halogen bond donor groups into macrocyclic and interlocked host systems can dramatically influence their anion recognition behaviour.[15,19,20] However, Table 1 shows the bis-iodotriazole [2]rotaxane **1e** exhibits the same trend in anion selectivity, *i.e.* chloride > bromide > iodide > dihydrogen phosphate, although it is noteworthy that a large reduction in association constant magnitude is observed for all halides, and a smaller degree of chloride selectivity is obtained compared to the prototriazole-

§ Within experimental error, the same association constant values were determined using titration data from monitoring protons *a*, *b*, *m* and those of the axle prototriazole units.

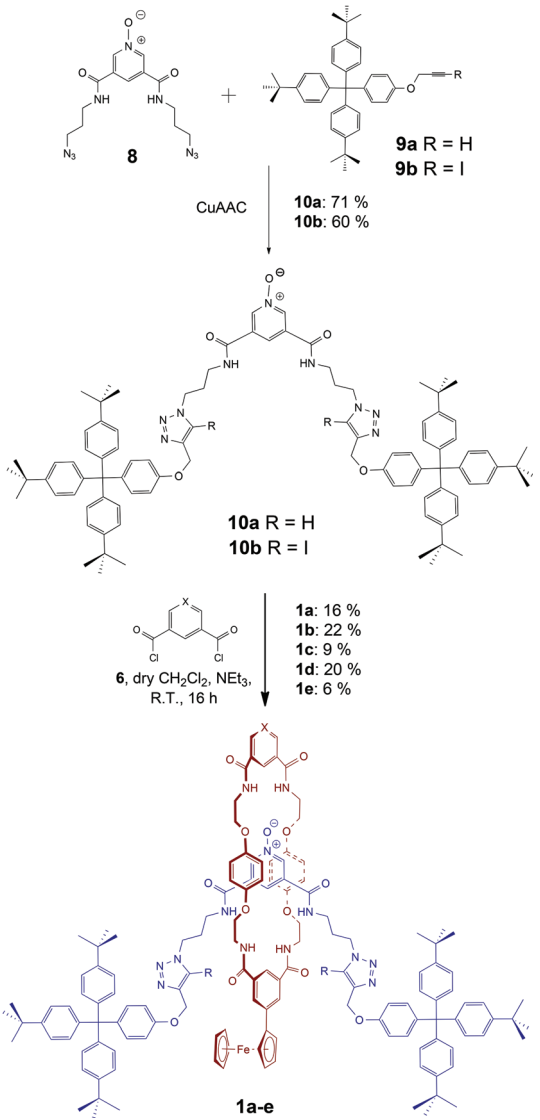

Scheme 2 Synthesis of neutral [2]rotaxanes *via* the amide condensation methodology.

bearing rotaxane analogues. This may be a consequence of the bulky triazole iodine atoms of the axle sterically hindering the entry of halides into the interlocked binding cleft of **1e**, which decreases the rotaxane's anion binding affinity.

Electrochemical anion sensing. The electrochemical anion recognition properties of rotaxanes **1a–e** and ferrocene-appended macrocycle **7a** were investigated by cyclic voltammetry in the electrolyte solution of 0.1 M $TBAPF_6$ in 1 : 1 CH_2Cl_2–CH_3CN with $Ag/AgNO_3$ reference electrode.[21] ¶

[2]Rotaxanes **1a–e** demonstrated electrochemical quasi-reversibility of the Fc/Fc^+ redox couple (see ESI†), with $E_{1/2}$ values of between +207 and +219 mV being obtained with respect

¶Prior to utilising the $Ag/AgNO_3$ working electrode, a ^1H NMR titration experiment was performed in the presence of $TBANO_3$ and [2]rotaxane **1b** (solutions prepared as described in Section S3). The results obtained indicated that the nitrate anion does not bind in the cavity of the rotaxanes (see ESI†).

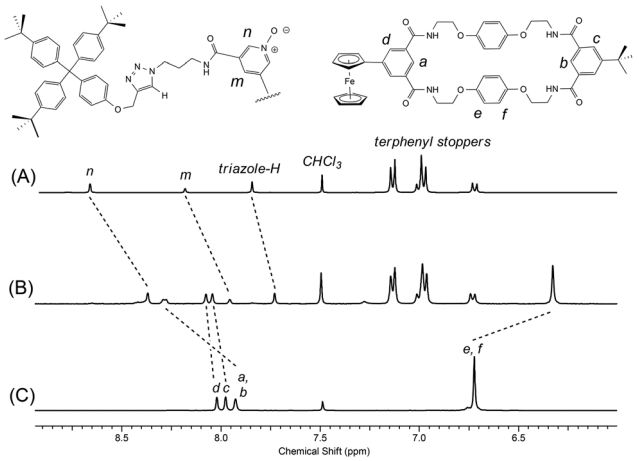

Fig. 2 Partial ^1H-NMR spectra of (A) proto-triazole axle **10a**; (B) [2]rotaxane **1a**; and (C) macrocycle **7a** (500 MHz, 1 : 1 $CDCl_3$–CD_3OD, 298 K).

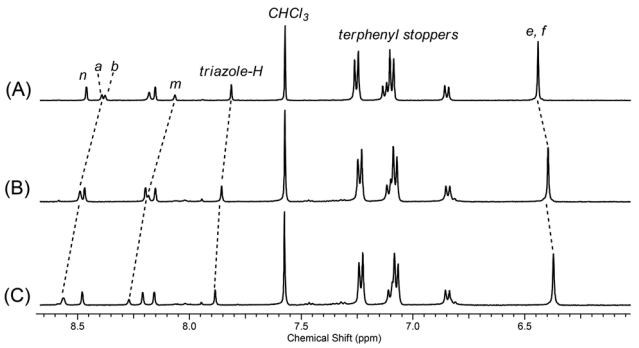

Fig. 3 ^1H-NMR of [2]rotaxane **1a** with (A) no TBACl present; (B) 1.0 equivalent of TBACl; (C) 2.0 equivalents of TBACl present (500 MHz, 45 : 45 : 10 $CDCl_3$–CD_3OD–D_2O, 298 K, [host] = 1.5 mM). Proton labels follow those in Fig. 2.

to the $Ag/AgNO_3$ reference electrode as shown in Table 2. As expected when taking account of the neutral pyridine *N*-oxide axle component, their $E_{1/2}$ values were very similar to that of macrocycle **7a**, unlike a previously-reported cationic ferrocene-appended pyridinium axle-based [2]rotaxane.[22]

In the presence of increasing quantities of chloride, a cathodic shift of the Fc/Fc^+ redox couple was observed for [2]rotaxane **1a** (Fig. 5 and Table 3). This is consistent with halide binding within the rotaxane's interlocked cavity stabilising the ferrocenium oxidation state, presumably *via* a through-bond mechanism, resulting in an enhanced binding affinity of chloride.[23] A significant cathodic shift of 27 mV was observed in the presence of 1.0 equivalent of chloride, which increased to 37 mV upon addition of a further 4 equivalents. In contrast, macrocycle **7a** displayed smaller cathodic shifts of 14 mV and 31 mV with 1.0 and 5.0 equivalents of chloride respectively. Bromide elicited a smaller cathodic shift with [2]rotaxane **1a** compared to chloride (Fig. 6 and Table 3), which can be attributed to the larger and more charge-diffuse nature of the halide anion. However, a loss of electrochemical reversibility was

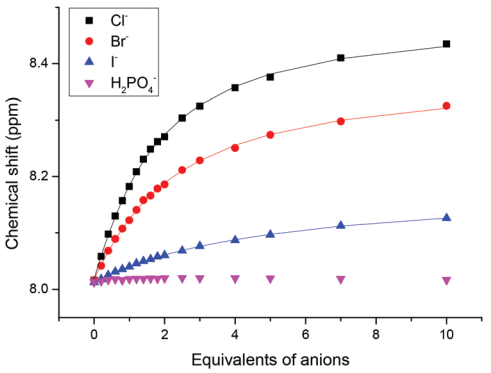

Fig. 4 Binding isotherms of anion titrations for [2]rotaxane **1a** with different TBA salts. The chemical shift of the internal isophthalamide proton of the pyridine *N*-oxide axle component is plotted as a function of equivalents of TBA salts added. Identical binding isotherms were obtained monitoring macrocycle component protons a and b and the axle prototriazole signal (500 MHz, 45 : 45 : 10 $CDCl_3$–CD_3OD–D_2O, 298 K, [host] = 1.5 mM).

Table 1 Association constants, K_a (M^{-1}), for [2]rotaxanes **1a–e** with various halide anions[a]

	1a	1b	1c	1d	1e
Cl^-	546(10)	423(13)	569(12)	542(16)	152(5)
Br^-	373(15)	259(20)	346(16)	376(13)	133(5)
I^-	138(5)	120(16)	124(3)	149(9)	81(8)

[a] Anions added as their TBA salts, temperature = 298 K, solvent: 45 : 45 : 10 $CDCl_3$–CD_3OD–D_2O, 298 K, values quoted have units of M^{-1}. The errors associated with each (<15%) are quoted in parentheses. $H_2PO_4^-$ and acetate did not bind to any of the rotaxanes investigated.

Table 2 $E_{1/2}$ values of [2]rotaxanes **1a–e** and macrocycle **7a**[a]

	1a	1b	1c	1d	1e	7a
$E_{1/2}$/mV	+211	+212	+207	+212	+219	+204

[a] Electrolyte: 0.1 M $TBAPF_6$ in 1 : 1 CH_2Cl_2–CH_3CN. Values are reported with respect to the $Ag/AgNO_3$ reference electrode at T = 293 K.

observed with the disappearance of the CV reduction wave in the presence of more than 1.0 equivalent of the oxoanions acetate and $H_2PO_4^-$. This suggested that an EC mechanism was in operation where formation of the ferrocenium moiety following electrochemical oxidation led to its rapid consumption by reacting with the oxoanions to form an unknown redox-stable species.‖ A similar loss of electrochemical reversibility, *via* an EC pathway, was observed with macrocycle **7a** as well (see ESI†). Notably, Table 3 shows that amongst all the

‖ Further evidence of a chemical change to the ferrocene moiety, following the occurrence of an EC mechanism, was provided when electrochemical reversibility was not restored upon titrating an excess of chloride anions into the oxoanion-**1a** electrochemical mixture, in spite of the rotaxane's preference for binding chloride.

Table 3 Comparison of the shifts in the Fc/Fc^+ redox couple of tetrabutyl-functionalised macrocycle **7a** and [2]rotaxane **1a** upon anion addition[a]

	$\Delta E_{1/2}$ for **7a**/mV		$\Delta E_{1/2}$ for **1a**/mV	
	1.0 eq.	5.0 eq.	1.0 eq.	5.0 eq.
Cl^-	−14	−31	−27	−37
Br^-	−9	−21	−16	−25
Acetate	−5	[b]	−19	[b]
$H_2PO_4^-$	[b]	[b]	−34	[b]

[a] Anions added as TBA salts. Electrolyte: 0.1 M $TBAPF_6$ in 1 : 1 CH_2Cl_2–CH_3CN. Reference electrode: $Ag/AgNO_3$; working electrode: glassy carbon; counter electrode: platinum. T = 293 K. [b] Not possible to determine $E_{1/2}$ after anion addition due to loss of reversibility and redox peaks.

anions investigated, chloride gave the largest cathodic shift, which correlates with the rotaxane's ^1H NMR-determined selectivity trend (Table 1).

Similar magnitudes of chloride anion-induced cathodic perturbations for all the prototriazole-bearing[2]rotaxanes **1b–d** were observed (Table 4). In spite of the bis-iodotriazole-bearing [2]rotaxane **1e** exhibiting notably weaker chloride anion binding than its prototriazole analogues (Table 1), comparable cathodic perturbations were observed (Table 4). When compared with previously-reported *charged* [2]rotaxane[22] and [2]catenane[11] systems bearing the same 5-ferrocene isophthalamide motif immediately adjacent to the interlocked anion binding site on the macrocycle component, it is noteworthy that the cathodic perturbations observed with chloride are of similar magnitude to the cathodic shifts exhibited by the *neutral* rotaxane systems reported here. This indicates that the binding enhancement factor (BEF) of this series of *neutral* [2]rotaxanes following oxidation of the ferrocene moiety is dictated by the through-bond communicative distance between the interlocked binding site and the ferrocene reporter group.

Conclusions

A series of novel *neutral* redox-active ferrocene functionalised [2]rotaxanes have been synthesised *via* chloride-templated clipping of bis-isophthalamide macrocycles around a pyridine *N*-oxide axle component. Following chloride template removal, ^1H NMR titration experiments revealed that the rotaxanes exhibit chloride selectivity over the heavier halides and oxoanions such as dihydrogen phosphate and acetate in competitive aqueous solvent media due to host–guest size-complementarity. Incorporating halogen bond-donors in the form of iodotriazole units into the rotaxane axle component diminished the halide anion binding affinity of the rotaxane which may be rationalised on steric grounds. Electrochemical voltammetric anion sensing investigations demonstrated the neutral rotaxane hosts to be capable of detecting chloride *via* significant cathodic perturbations of the rotaxanes' ferrocene/ferrocenium redox-couple.

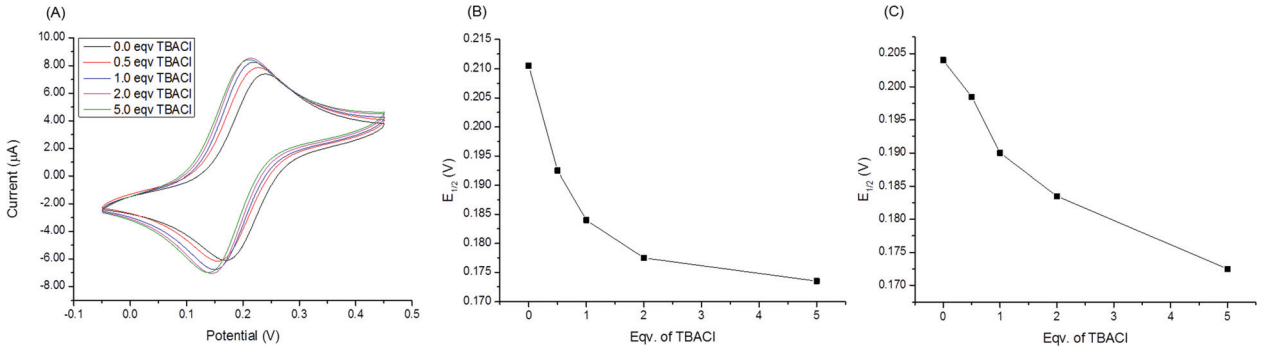

Fig. 5 (A) CVs of [2]rotaxane **1a** in 0.1 M $TBAPF_6$ (1 : 1 CH_2Cl_2–CH_3CN) with increasing equivalents of TBACl added. (B) Plot of the half-wave potential ($E_{1/2}$) of **1a** in the presence of different aliquots of TBACl. (C) Plot of half-wave potential ($E_{1/2}$) of **7a** with increasing quantities of TBACl added.

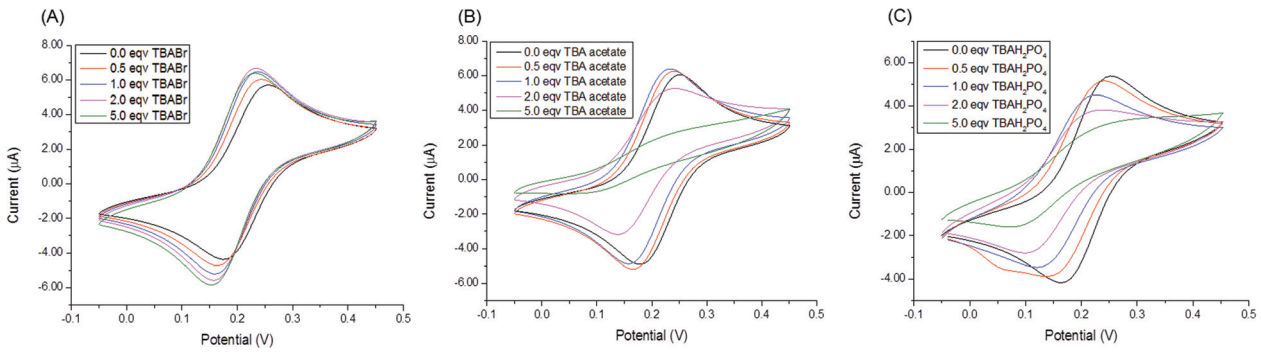

Fig. 6 CVs of [2]rotaxane **1a** in the presence of increasing aliquots of (A) TBABr; (B) TBA acetate; and (C) $TBAH_2PO_4$.

Table 4 Shifts in redox couple of Fc/Fc^+ of [2]rotaxanes **1a–e** upon addition of TBACl[a]

	$\Delta E_{1/2}$/mV	
	After 1.0 eq.	After 5.0 eq.
1a	−27	−37
1b	−25	−34
1c	−20	−24
1d	−25	−33
1e	−20	−31

[a] Electrolyte: 0.1 M $TBAPF_6$ in 1 : 1 CH_2Cl_2–CH_3CN. Reference electrode: $Ag/AgNO_3$; working electrode: glassy carbon; counter electrode: platinum wire. T = 293 K.

Acknowledgements

J.Y.C.L thanks the Agency for Science, Technology and Research (A*STAR), Singapore, for a postgraduate scholarship. M. J. C. thanks the European Research Council for funding under the European Union's Framework Program (FP7/2007-2013) ERC Advanced Grant Agreement number 267426.

Notes and references

1 J. L. Sessler, P. A. Gale and W. C. Cho, *Anion Receptor Chemistry*, Royal Society of Chemistry, 2006.
2 A. Caballero, F. Zapata and P. D. Beer, *Coord. Chem. Rev.*, 2013, **257**, 2434–2455.
3 P. A. Gale, N. Busschaert, C. J. E. Haynes, L. E. Karagiannidis and I. L. Kirby, *Chem. Soc. Rev.*, 2014, **43**, 205–241.
4 E. R. Kay, D. A. Leigh and F. Zerbetto, *Angew. Chem., Int. Ed.*, 2007, **46**, 72–191.
5 S. F. M. van Dongen, S. Cantekin, J. A. A. W. Elemans, A. E. Rowan and R. J. M. Nolte, *Chem. Soc. Rev.*, 2014, **43**, 99–122.
6 M. J. Langton and P. D. Beer, *Acc. Chem. Res.*, 2014, **47**, 1939–1949.
7 L. M. Hancock, E. Marchi, P. Ceroni and P. D. Beer, *Chem. – Eur. J.*, 2012, **18**, 11277–11283.
8 N. G. White, S. Carvalho, V. Felix and P. D. Beer, *Org. Biomol. Chem.*, 2012, **10**, 6951–6959.
9 J. M. Mercurio, F. Tyrrell, J. Cookson and P. D. Beer, *Chem. Commun.*, 2013, **49**, 10793–10795.
10 A. Caballero, N. G. White and P. D. Beer, *Angew. Chem., Int. Ed.*, 2011, **50**, 1845–1848.
11 N. H. Evans, H. Rahman, A. V. Leontiev, N. D. Greenham, G. A. Orlowski, Q. Zeng, R. M. J. Jacobs, C. J. Serpell, N. L. Kilah, J. J. Davis and P. D. Beer, *Chem. Sci.*, 2012, **3**, 1080–1089.
12 D. E. Phipps and P. D. Beer, *Tetrahedron Lett.*, 2009, **50**, 3454–3457.
13 F. Zapata, O. A. Blackburn, M. J. Langton, S. Faulkner and P. D. Beer, *Chem. Commun.*, 2013, **49**, 8157–8159.

14 V. Aucagne, K. D. Hänni, D. A. Leigh, P. J. Lusby and D. B. Walker, *J. Am. Chem. Soc.*, 2006, **128**, 2186–2187.
15 N. L. Kilah, M. D. Wise, C. J. Serpell, A. L. Thompson, N. G. White, K. E. Christensen and P. D. Beer, *J. Am. Chem. Soc.*, 2010, **132**, 11893–11895.
16 N. H. Evans, C. J. Serpell and P. D. Beer, *Chem. Commun.*, 2011, **47**, 8775–8777.
17 M. J. Hynes, *J. Chem. Soc., Dalton Trans.*, 1993, 311–312.
18 F. P. Schmidtchen, *Chem. Soc. Rev.*, 2010, **39**, 3916–3935.
19 A. Caballero, F. Zapata, N. G. White, P. J. Costa, V. Félix and P. D. Beer, *Angew. Chem., Int. Ed.*, 2012, **51**, 1876–1880.
20 L. C. Gilday, N. G. White and P. D. Beer, *Dalton Trans.*, 2013, **42**, 15766–15773.
21 B. Kratochvil, E. Lorah and C. Garber, *Anal. Chem.*, 1969, **41**, 1793–1796.
22 N. H. Evans and P. D. Beer, *Org. Biomol. Chem.*, 2011, **9**, 92–100.
23 P. D. Beer, P. A. Gale and G. Z. Chen, *J. Chem. Soc., Dalton Trans.*, 1999, 1897–1910.